

Mutagenesis study on amino acids around the molybdenum centre of the periplasmic nitrate reductase from *Ralstonia eutropha*[☆]

Thomas Hettmann,^a Roman A. Siddiqui,^a Christa Frey,^a Teresa Santos-Silva,^b Maria João Romão,^b and Stephan Diekmann^{a,*}

^a Institute for Molecular Biotechnology, Beutenbergstr. 11, 07745 Jena, Germany

^b REQUIMTE, CQFB, Departamento de Química, FCT, Universidade Nova de Lisboa, 2829-516 Caparica, Portugal

Received 14 June 2004
Available online 2 July 2004

Abstract

Molybdenum enzymes containing the pterin cofactor are a diverse group of enzymes that catalyse in general oxygen atom transfer reactions. Aiming at studying the amino acid residues, which are important for the enzymatic specificity, we used nitrate reductase from *Ralstonia eutropha* (*R.e.*NAP) as a model system for mutational studies at the active site. We mutated amino acids at the Mo active site (Cys181 and Arg421) as well as amino acids in the funnel leading to it (Met182, Asp196, Glu197, and the double mutant Glu197-Asp196). The mutations were made on the basis of the structural comparison of nitrate reductases with formate dehydrogenases (FDH), which show very similar three-dimensional structures, but clear differences in amino acids surrounding the active site. For mutations Arg421Lys and Glu197Ala we found a reduced nitrate activity while the other mutations resulted in complete loss of activity. In spite of the partial or total loss of nitrate reductase activity, these mutants do not, however, display FDH activity.

© 2004 Elsevier Inc. All rights reserved.

Keywords: Nitrate reductase; Formate dehydrogenase; Oxidoreductases; Molybdopterin; *Ralstonia eutropha*

Denitrification is a microbial process ubiquitous among bacteria, in which nitrate is used as an alternative electron acceptor for energy production. Two types of dissimilatory nitrate reductases, localized in either the membrane or the periplasm, have been described in bacteria. The membrane-bound nitrate reductase (NAR) catalyses nitrate reduction, with concomitant generation of proton motive force under anaerobic conditions [1,2]. Various roles have been described for the periplasmic nitrate reductase (NAP): (i) it partici-

pates in cellular redox balancing by which nitrate is used as an electron sink to dissipate excess reducing power, (ii) it is responsible for initiating aerobic denitrification, and (iii) it also fulfils a nitrate scavenging role [3].

Many oxidoreductases contain transition metals at their active site. Molybdenum and tungsten are present in biological systems as part of the nitrogenase cofactor or bound to the organic cofactor pyranopterin. The molybdopterin or pyranopterin class of enzymes is very diverse and has been subdivided into three main families [4]: the xanthine oxidase family, the sulphite oxidase family, and the DMSO reductase family. With the exception of the eukaryotic assimilatory nitrate reductases, which are part of the sulphite oxidase family, nitrate reductases belong to the DMSO reductase family of Mo enzymes. Within the variety of enzymes belonging to this family, the periplasmic dissimilatory/respiratory nitrate reductases (NAP) as well as the formate dehydrogenases (FDH) share the highest degree of structural similarity in terms of their three-dimensional structures.

[☆] Abbreviations: BSA, bovine serum albumin; *D.*, *Desulfovibrio*; DMSOR, dimethyl sulphoxide reductase; FDH, formate dehydrogenase; FDH-H, formate dehydrogenase component of the formate-hydrogen lyase complex of *E. coli*; FDH-N, nitrate-dependent formate dehydrogenase of *E. coli* when growing anaerobically on nitrate; MGD, molybdopterin guanine dinucleotide; Moco, pyranopterin-ene-1,2-dithiolate cofactor or molybdopterin; NAP, periplasmic nitrate reductase; NAR, membrane-bound nitrate reductase.

* Corresponding author. Fax: +49-3641-656261.

E-mail address: diekmann@imb-jena.de (S. Diekmann).

So far, only three crystal structures of a periplasmic nitrate reductase have been solved: (i) the monomeric *D.d.*NAP, isolated from the sulphate reducer *Desulfovibrio (D.) desulfuricans (d.)* ATCC 27774 reported in 1999 at 1.9 Å resolution [5,6], (ii) a proteolytic fragment of the β -subunit of the heterodimeric NAP-AB from *Haemophilus influenzae* [7], and recently (iii) the heterodimeric NAP-AB complex of *Rhodobacter sphaeroides* at 3.2 Å resolution [8]. Three crystal structures are currently available for formate dehydrogenases: The FDH-H (part of the hydrogen lyase complex) from *Escherichia coli* [9], the membrane protein FDH-N (expressed when growing anaerobically on nitrate) from *E. coli* [10], and the W-containing *Desulfovibrio gigas* formate dehydrogenase (*D.g.*W-FDH) [11,12].

While *D.d.*NAP and *E. coli* FDH-H are monomeric enzymes consisting of 723 and 715 amino acids (aa), respectively, the *D.g.*W-FDH is a heterodimeric enzyme with 977 aa (α -) and 214 aa (β -subunit), and the *E. coli* FDH-N forms a trimeric complex of three subunits of 982 aa (α -), 290 aa (β -), and 217 aa (γ -subunit), which associate as trimers along the membrane. The structures of *D.d.*NAP and *E. coli* FDH-H are functionally related to the large catalytic α -subunit of *D.g.*W-FDH and of *E. coli* FDH-N. These catalytic α -subunits carry the molybdopterin cofactor (W/Mo[(MGD)₂, -SH/-OH, -SeCys] and Mo[(MGD)₂, -OH, -Cys] for FDHs and NAPs, respectively) as well as one [4Fe-4S] cluster. Although differing in their molecular weights, their structures can be superimposed showing that their respective core structures are quite similar. The superposition of the large subunit of *D.g.*W-FDH with NAP shows an r.m.s. deviation of 2.0 Å for 636 C α atoms, while the comparison with *E. coli* FDH-H gives a corresponding r.m.s. deviation of 2.1 Å for 659 C α atoms [12]. The structure of the α -subunit of the *E. coli* FDH-N is superimposable with that from *E. coli* FDH-H with an r.m.s. deviation of 1.9 Å for 599 C α atoms [10]. The classification of these homologous proteins in terms of the topology is also similar and the overall structure can be subdivided into four domains, two of which correspond to non-contiguous stretches of the polypeptide chain. In the larger proteins *E. coli* FDH-N and *D.g.*W-FDH, the additional residues of the catalytic α -subunit are essentially distributed over the molecular surface as insertions in the whole polypeptide.

The differences between both kinds of enzymes (NAP and FDH) that account for their different substrate specificities (reduction of nitrate to nitrite or conversion of formate into carbon dioxide) are localized essentially in the vicinity of the Mo active site as well as in the tunnel leading to it [6].

Recently, the first crystal structure of the membrane-bound quinol-nitrate oxidoreductases (NAR-GHI) from *E. coli* was solved by two independent groups [1,2]. Although with a common architecture of the catalytic

subunit (NAR-G) this nitrate reductase shows a greater structural difference in the active site and surrounding regions as well as in the tunnel leading to the active site when compared to periplasmic nitrate reductases or formate dehydrogenases. The NAR-structure revealed several, however, novel and interesting aspects, since for the first time an aspartate (Asp222) amino acid residue is coordinated to the Mo. Besides, in one of the reported structures [1], one of the MGD cofactors (MGD-Q) is present in a bicyclic dihydropterin structure rather than the tricyclic pyranopterin structure found so far in all Mo enzymes.

Based on these structural similarities and differences, we became interested in elucidating the role of the various amino acids of periplasmic nitrate reductases in (i) taking part in the reaction mechanism and in (ii) determining the substrate specificity. In particular we studied Cys181 that directly coordinates the Mo atom as well as amino acids in the active site cavity (Met182, Glu197, Asp196, and Arg421). The mutations (Arg421Lys) and (Glu197Ala) showed a reduced activity while all other mutations showed no nitrate reductase activity. The mutations in the funnel were aimed to change the nitrate reductase towards the structurally very similar formate dehydrogenase (FDH). We also tested for FDH activity but found none.

Materials and methods

Bacterial strains and plasmids. The genes for the periplasmic nitrate reductase of *Ralstonia eutropha* are not part of the bacterial chromosome but located on the 450-kb megaplasmid pHG1 [13]. For our mutation studies we used strain HF210 [14], the megaplasmid-free derivative of the wild-type strain H16 (DSM 428, ATCC 17699), together with plasmids containing the complete *nap* cluster (pGE49, pCH332, pNapBC, pTH100, and pTH200) [15,16]. A complete list of bacterial strains and plasmids used in this study is given in Table 1.

Media and growth conditions. *Ralstonia eutropha* strains were grown aerobically at 30 °C with 0.4% (wt/vol) fructose as carbon source and 0.2% ammonium chloride (wt/vol) as nitrogen source in 100 ml mineral medium as described in [15,17]. Strains of *E. coli* were grown at 37 °C in Luria-Bertani medium [18]. Solid media contained 1.8% (wt/vol) agar. Antibiotics were added as appropriate for *R. eutropha* (tetracycline, 12.5 µg/ml) and for *E. coli* (tetracycline, 12.5 µg/ml; ampicillin, 100 µg/ml). Cell growth was monitored by measuring the optical density at 600 nm.

Mutation and cloning protocol. The mutation and cloning procedures follow the same strategy as described in [16]. The complete *nap* clustering with the genes *napE*, *napD*, *napA*, *napB*, and *napC* (total length 5.8 kb) was recloned into the vector pBC SK+ (Stratagene) and subcloned in pMCS5 (MoBiTec, Göttingen, Germany) to yield the vector pNapBC and pNap100, respectively [16]. A 3.1-kb subfragment of the *nap* cluster was excised from vector pNapBC with the restriction endonucleases *EcoRI* and *NsiI* to yield vector pNapNE. A *NsiI* restriction site in the multi-cloning site of pNap100 interfering with one part of the cloning strategy was removed by digestion with the restriction endonucleases *EcoRV* and *HpaI* and subsequent religation yielding in vector pNap100 Δ .

A small part of the *nap* cluster was amplified by PCR with Herculanse (Stratagene) or DyNAzyme EXT DNA Polymerase (Finnzymes,

Table 1
Bacterial strains, vectors, and oligonucleotides

| Strain, plasmid or oligonucleotide | Relevant characteristics | Reference or source |
|------------------------------------|---|--------------------------------|
| <i>R. eutropha</i> | | |
| H16 | Nar ⁺ , Nas ⁺ , Nap ⁺ , pHG1 ⁺ | DSM 428, ATCC 17699 |
| HF210 | Nar ⁺ , Nas ⁺ , Nap ⁻ pHG1 ⁻ ; derivative of H16 | [14] |
| <i>E. coli</i> | | |
| DH5 α | F ⁻ ϕ 80d <i>lacZ</i> Δ M15 Δ (<i>lacZYA-argF</i>) U169 <i>deoR recA1 endA1 hsdR17</i> (r _k ⁻), m _k ⁺ <i>phoA supE44</i> λ ⁻ <i>thi-1 gyrA96 relA1</i> | Invitrogen |
| S17-1 | Tra ⁺ <i>recA pro thi hsdR chr::RP4-2</i> | [28] |
| Plasmids | | |
| pBC SK+ | Cm ^R <i>lacZ'</i> <i>flori</i> ColE1 <i>ori</i> ; T3 promoter, T7 promoter | Stratagene |
| pBluescript SK+ | Ap ^R <i>lacZ'</i> <i>flori</i> ColE1 <i>ori</i> ; T3 promoter, T7 promoter | Stratagene |
| pMCS5 | Ap ^R <i>lacZ'</i> <i>flori</i> pBR322 <i>ori</i> ; T7 promoter | MoBiTec, Göttingen, Germany |
| pCR 2.1-TOPO | Ap ^R Km ^R <i>lacZ'</i> pUC <i>ori</i> <i>flori</i> ; T7 promoter | Invitrogen |
| pCM62 | Broad-host-range vector, Tc ^R <i>lacZ'</i> <i>traJ'</i> ColE1 <i>ori</i> <i>oriV</i> <i>oriT</i> | [19] |
| pVK102 | Km ^R Tc ^R Mob ⁺ RP4 <i>ori</i> | [29] |
| pGE49 | 16-kb <i>Hind</i> III fragment of megaplasmid pHG1 in pVK102 | [15] |
| pCH332 | 6.0-kb <i>EcoRV</i> – <i>Clal</i> fragment of pGE49 in pBluescript SK+ | [15] |
| pNapBC | 6.0-kb <i>EcoRV</i> – <i>Clal</i> fragment of pGE49 in pBC SK+ | [16] |
| pNapNE | 3.1-kb <i>EcoRI</i> – <i>NsiI</i> fragment of pNapBC in pMCS5 | This study |
| pTH100 | 6.0-kb <i>EcoRV</i> – <i>XhoI</i> fragment of pNapBC in pMCS5 | [16] |
| pTH100 Δ | A 12-bp fragment of pTH100 has been removed by digestion with <i>EcoRV</i> and <i>HpaI</i> (blunt-end cutters) and subsequent religation. As a consequence the restriction sites for <i>EcoRV</i> , <i>NsiI</i> , and <i>HpaI</i> are destroyed | This study |
| pTH200 | 6.1-kb <i>SwaI</i> – <i>SmaI</i> fragment of pTH100 in pCM62 | [16] |
| pTOPO-DEGA | 1.2-kb PCR-product DEGA in pCR 2.1-TOPO | This study |
| pTOPO-D196G | 1.2-kb PCR-product D196G in pCR 2.1-TOPO | This study |
| pTOPO-E197A | 1.2-kb PCR-product E197A in pCR 2.1-TOPO | This study |
| pTOPO-M182H | 1.2-kb PCR-product M182H in pCR 2.1-TOPO | This study |
| pTOPO-C181S | 1.2-kb PCR-product C181S in pCR 2.1-TOPO | This study |
| pTOPO-R421E | 0.5-kb PCR-product R421E in pCR 2.1-TOPO | This study |
| pTOPO-R421K | 0.5-kb PCR-product R421K in pCR 2.1-TOPO | This study |
| pTH103 | 986-bp <i>BglII</i> – <i>EcoRI</i> fragment of pTOPO-DEGA in pTH100 | This study |
| pTH104 | 986-bp <i>BglII</i> – <i>EcoRI</i> fragment of pTOPO-D196G in pTH100 | This study |
| pTH105 | 986-bp <i>BglII</i> – <i>EcoRI</i> fragment of pTOPO-E197A in pTH100 | This study |
| pTH106 | 986-bp <i>BglII</i> – <i>EcoRI</i> fragment of pTOPO-M182H in pTH100 | This study |
| pTH107 | 986-bp <i>BglII</i> – <i>EcoRI</i> fragment of pTOPO-C181S in pTH100 | This study |
| pNapNE-R421E | 315-bp <i>EcoRI</i> – <i>BstEII</i> fragment of pTOPO-R421E in pNapNE | This study |
| pTH108 | 3.1-kb <i>EcoRI</i> – <i>NsiI</i> fragment of pNapNE-R421E in pTH100 Δ | This study |
| pNapNE-R421K | 315-bp <i>EcoRI</i> – <i>BstEII</i> fragment of pTOPO-R421K in pNapNE | This study |
| pTH109 | 3.1-kb <i>EcoRI</i> – <i>NsiI</i> fragment of pNapNE-R421K in pTH100 Δ | This study |
| pTH203 | 6.1-kb <i>SwaI</i> – <i>SmaI</i> fragment of pTH103 (pNapS5-DEGA) in pCM62 | This study |
| pTH204 | 6.1-kb <i>SwaI</i> – <i>SmaI</i> fragment of pTH104 (pNapS5-D196G) in pCM62 | This study |
| pTH205 | 6.1-kb <i>SwaI</i> – <i>SmaI</i> fragment of pTH105 (pNapS5-E197A) in pCM62 | This study |
| pTH206 | 6.1-kb <i>SwaI</i> – <i>SmaI</i> fragment of pTH106 (pNapS5-M182H) in pCM62 | This study |
| pTH207 | 6.1-kb <i>SwaI</i> – <i>SmaI</i> fragment of pTH107 (pNapS5-C181S) in pCM62 | This study |
| pTH208 | 6.1-kb <i>SwaI</i> – <i>SmaI</i> fragment of pTH108 (pNapEHAS5-R421E) in pCM62 | This study |
| pTH209 | 6.1-kb <i>SwaI</i> – <i>SmaI</i> fragment of pTH109 (pNapEHAS5-R421K) in pCM62 | This study |
| Oligonucleotides | | |
| <i>BglII</i> -100-sense | 5'-AC CTC ACC TGC CTC CAC CAG-3'; position 965–984 | [16] |
| <i>EcoRI</i> + 100-anti | 5'-TGG GGT CGG CGT ACA GTT CG-3'; position 2156–2137 | [16] |
| <i>EcoRI</i> -100-sense | 5'-C GTG ACC GAC ATC GGC TAC G-3'; position 1951–1970 | This study |
| <i>BstEII</i> + 100-anti | 5'-GC ATG CGG TTC TGC AGC ACG-3'; position 2471–2452 | This study |
| DEGA-sense | 5'-TTC GGC ATG <u>GGC</u> GCC CCG ATG GGC TGC TAT-3'; position 1637–1666 | This study |
| DEGA-anti | 5'-A GCC CAT CGG <u>GGC</u> GCC CAT GCC GAA GGT GC-3'; position 1661–1632 | This study |
| D196G-sense | 5'-TTC GGC ATG <u>GGC</u> GAG CCG ATG GGC TG-3'; position 1637–1662 | This study |
| D196G-anti | 5'-CAT CGG CTC <u>GCC</u> CAT GCC GAA GGT GC-3'; position 1657–1632 | This study |
| E197A-sense | 5'-GGC ATG GAC <u>GCG</u> CCG ATG GGC TGC TA-3'; position 1640–1665 | This study |
| E197A-anti | 5'-GCC CAT CGG <u>GCG</u> GTC CAT GCC GAA GG-3'; position 1660–1635 | This study |
| M182H-long | 5'-G CGG CAT TGC <u>CAT</u> GCA TCG GCC GCG GCC GGC TTC AT-3'; position 1594–1629 | This study |

Table 1 (continued)

| Strain, plasmid or oligonucleotide | Relevant characteristics | Reference or source |
|------------------------------------|--|---------------------|
| M182H-anti | 5'-C GGC CGA TGC <u>ATG</u> GCA ATG CCG CGC ATT-3'; position 1616–1589 | This study |
| C181S-sense | 5'-GCG CGG CAT <u>TCC</u> ATG GCA TCG GCC GC-3'; position 1592–1617 | This study |
| C181S-anti | 5'-CGA TGC CAT <u>GGA</u> ATG CCG CGC ATT GG-3'; position 1612–1587 | This study |
| R421E-sense | 5'-C GGC ACC GCG <u>GAG</u> GAG GTC GGC ACC TTC-3'; position 2311–2338 | This study |
| R421E-anti | 5'-T GCC GAC CTC <u>CTC</u> CGC GGT GCC GCA GGC-3'; position 2333–2306 | This study |
| R421K-sense | 5'-C GGC ACC GCG <u>AAG</u> GAG GTC GGC ACC TTC-3'; position 2311–2338 | This study |
| R421K-anti | 5'-T GCC GAC CTC <u>CTT</u> CGC GGT GCC GCA GGC-3'; position 2333–2306 | This study |

In the oligonucleotide sequences, the base triplets coding for the amino acids to be exchanged are underlined. Bases in the mutated sequence that differ from the wild-type sequence are shown in grey.

Espoo, Finland). For primers used in this study, see Table 1. The amplified DNA fragment was either 1192 bp long (primer pair *Bgl*III-100-sense and *Eco*RI+100-anti) or 521 bp (primer pair *Eco*RI-100-sense and *Bst*EII+100-anti). During the amplification, mutations were introduced at particular sites by PCR mutagenesis leading to the wanted single or double amino acid replacements (D196G-E197A, D196G, E197A, M182H, C181S, R421K, and R421E). The sequence and position of the oligonucleotides are listed in Table 1. The modified codons are underlined. The sequence of the oligonucleotide *Bgl*III-100-sense is located on the sense strand of the *napA* gene (position 965–984) about 100 nucleotides upstream of a *Bgl*III restriction site (position 1065), while the sequence of the oligonucleotide *Eco*RI+100-anti is located on the anti-sense strand of the *napA* gene (position 2137–2156) about 100 bp downstream of an *Eco*RI restriction site (position 2051). The sequence of the oligonucleotide *Eco*RI-100-sense is located on the sense strand of the *napA* gene (position 1951–1970) about 100 nucleotides upstream of an *Eco*RI restriction site (position 2051), while the sequence of the oligonucleotide *Bst*EII+100-anti is located on the anti-sense strand of the *napA* gene (position 2471–2452) about 100 bp downstream of a *Bst*EII restriction site (position 2347).

The PCR products were introduced by TA cloning into the vector pCR 2.1-TOPO (Invitrogen, USA) to yield the plasmids pTOPO-DEGA, pTOPO-D196G, pTOPO-E197A, pTOPO-M182H, pTOPO-C181S, pTOPO-R421E, and pTOPO-R421K. The obtained mutated sequences were verified by DNA sequencing (MWG, Germany). The inserts carrying the mutations were excised from the vector by the restriction endonucleases *Bgl*III and *Eco*RI (exchanges D196G-E197A, D196G, E197A, M182H, and C181S) or by the restriction endonucleases *Eco*RI and *Bst*EII (exchanges R421E, R421K). The excised fragments were either ligated into the vector pTH100 (exchanges D196G-E197A, D196G, E197A, M182H, and C181S) replacing the wild-type *Bgl*III/*Eco*RI segment of the complete *nap* cluster to yield the vectors pTH103–pTH107; or they were ligated into the vector pNapNE (exchanges R421E, R421K) replacing the wild-type *Eco*RI/*Bst*EII segment of the 3.1-kb fragment of the *nap* cluster yielding the plasmids pNapNE-R421E and pNapNE-R421K. The 3.1-kb fragments carrying the mutation were excised from the plasmids pNapNE-R421E and pNapNE-R421K by digestion with the restriction endonucleases *Nsi*I and *Eco*RI and ligated into the vector pNap100Δ yielding in the plasmids pTH108 and pTH109, respectively. The correct arrangement of the inserts was verified by restriction analysis for each newly constructed plasmid.

The mutated *nap* cluster was cut out of the vector pTH103, pTH104, pTH105, pTH106, pTH107, pTH108, and pTH109 by the restriction endonucleases *Sma*I and *Swa*I and this blunt-ended fragment was cloned into the broad host range vector pCM62 [19] resulting in pTH203 (double exchange D196G-E197A), pTH204 (exchange D196G), pTH205 (exchange E197A), pTH206 (exchange M182H), pTH207 (exchange C181S), pTH208 (exchange R421E), and pTH209 (exchange R421K). The vector pCM62 had been treated with *Xba*I and the sticky ends had been filled by Klenow polymerase to yield blunt ends, too. Only those plasmids were chosen (named pTH203, pTH204, pTH205, pTH206, pTH207, pTH208, and pTH209) where the *nap*

cluster was in anti-sense orientation to the lac promoter of the vector pCM62.

The vector pCM62 can be replicated in *E. coli* as well as in *R. eutropha*. The vectors pTH203, pTH204, pTH205, pTH206, pTH207, pTH208, and pTH209 were transformed into the *E. coli* strain S17-1 and subsequently mobilized from *E. coli* strain S17-1 to *R. eutropha* strain HF210 according to [15].

The transconjugants of *R. eutropha* harboring either a *nap* cluster with mutation or a wild-type *nap* cluster on a plasmid were grown in 100 ml cultures and harvested in the stationary phase. Periplasmic fractions of *R. eutropha* were prepared as described in [20].

Enzyme activity and protein assays. Nitrate reductase activity was determined in the periplasmic extracts as well as in crude cell extracts with the microtitre plate assay described by Borchering et al. [21] with the modifications described in [16]. Protein concentrations were determined in an assay based on the Lowry method [22] with BSA as protein standard as detailed in [16].

Formate dehydrogenase activity assay was carried out using polyacrylamide native gel electrophoresis of the periplasmic extracts, with methyl viologen as the electron acceptor and sodium formate as the substrate. The gel was stained under argon atmosphere with a solution of 1 mM methyl viologen, 50 mM sodium formate, and 100 mM β-mercaptoethanol, at pH 5.5.

SDS-PAGE and Western blot. Denaturing polyacrylamide gel electrophoresis was performed according to the Laemmli method [23] with the variations as described in [16]. After electrophoresis, gels were stained with Coomassie brilliant blue R-250.

Gels used for Western blot analysis were not stained, but blotted on a PVDF membrane (Immobilon-P, Millipore) using a semi-dry blot apparatus (Fast Blot B-33, Biometra, Göttingen, Germany) as detailed in [16]. After blotting the gel was stained with Coomassie brilliant blue R-250 to check the completeness of the transfer. The PVDF membrane was blocked for 1 h with 5% skimmed milk powder in PBS-Tween (100 mM sodium phosphate buffer, pH 7.5, 100 mM NaCl, and 0.1% (wt/vol) Tween 20). The nitrate reductase was detected by a two-step incubation with antibodies, at first with an anti-serum from rabbit against purified nitrate reductase [20] diluted 1:1000 in PBS-Tween, second with goat-anti-rabbit IgG conjugated with peroxidase (Dianova, Hamburg, Germany) diluted 1:1000 in PBS-Tween. The colour reaction was performed with a solution of a few crystals of 3,3'-diamino-benzidine dissolved in 10 ml of 50 mM sodium acetate, pH 5.0, containing 0.03% H₂O₂. The relative intensity of the NAP-A bands on the blot was determined using the MacCAM 1.0b (Cybertech) software.

Sequence alignment. The primary sequence of the α-subunit from four periplasmic nitrate reductases and that of the α-subunit from three formate dehydrogenases were sequence aligned. The accession numbers of the amino acid sequences are: NP_942849 *R. eutropha* NAP-A; P33937 *E. coli* NAP-A; 2NAPA *D. desulfuricans* NAP-A; Q53176 *R. sphaeroides* NAP-A; P07658 *E. coli* FDH-H, α-subunit; P24183 *E. coli* FDH-N, α-subunit; and CAC86667 *D. gigas* W-FDH, α-subunit. These seven amino acid sequences (Fig. 2) were aligned using the ClustalW program [24]; at the web page of NPS@ [25].

Results

In order to study the activity and specificity of periplasmic nitrate reductase, we performed a mutagenesis study in our model system: nitrate reductase of *R. eutropha* (NAP). As the structural basis for our mutagenesis studies, we refer to the previously described [16] three-dimensional model of the catalytic subunit NAP-A.

The genes for the periplasmic nitrate reductase of *R. eutropha* strain H16 are not part of the bacterial

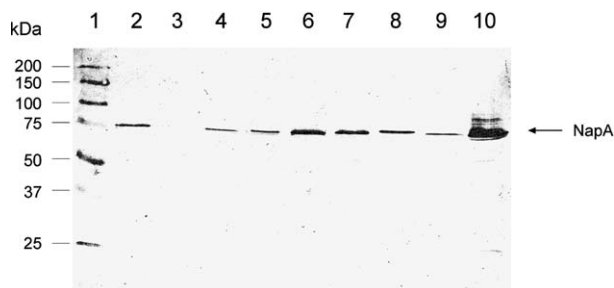


Fig. 1. Western blot analysis of periplasmic extracts from different *Ralstonia eutropha* strains. Lanes 2–10 each contain 15 μ g of periplasmic protein. Lane 1, Molecular weight standard (7.5 μ l Precision Plus Protein standard, dual colour, Bio-Rad); lane 2, strain HF210 harboring plasmid pTH200 (containing the wild-type *napEDABC* cluster); lane 3, *nap*-negative, megaplasmid-free strain HF210; lane 4, strain HF210 harboring plasmid pTH203 (like pTH200 but with double amino acid exchange D196G-E197A); lane 5, strain HF210 harboring plasmid pTH204 (like pTH200 but with single amino acid exchange D196G); lane 6, strain HF210 harboring plasmid pTH205 (like pTH200 but with single amino acid exchange E197A); lane 7, strain HF210 harboring plasmid pTH206 (like pTH200 but with single amino acid exchange M182H); lane 8, strain HF210 harboring plasmid pTH208 (like pTH200 but with single amino acid exchange R421E); lane 9, strain HF210 harboring plasmid pTH209 (like pTH200 but with single amino acid exchange R421K); and lane 10, strain HF210 harboring plasmid pTH207 (like pTH200 but with single amino acid exchange C181S).

chromosome but are located on the megaplasmid pHG1, the complete sequence of which was published recently [26]. We introduced the desired mutations into the *napA* gene by site-directed mutagenesis and used a periplasmic nitrate reductase negative and megaplasmid-free derivative of the wild-type H16, *R. eutropha* HF210, as the host to study the effect of the mutant enzymes. The nine strains studied (wild-type *napEDABC*, mutant C181S, mutant M182H, mutant D196G, mutant E197A, double mutant DEGA, mutant R421K, mutant R421E, and *nap*-negative strain HF210) were grown in 100 ml cultures in at least two to four independent experiments, harvested in the stationary phase, and the periplasm was isolated. Nitrate reductase activity was determined in whole cell and in periplasmic extracts but not in further purified form to avoid loss of activity during the four-step purification procedure (including ammonium sulphate precipitation, hydrophobic interaction and cation exchange chromatography, and gel filtration [15]) and to keep the enzyme in an “as native as possible” state. The activity assay was carried out with benzyl viologen (BV) as artificial electron donor. The presence of the enzymes in the periplasm, independent of their activity, was verified in every single case by Western blot analysis (see Fig. 1). All strains, except for the *nap*-deficient strain HF210, gave a clear NAP-A signal showing that the nitrate reductase is present in normal amounts in the periplasm. In separate gels, the NAP-B subunit was also clearly identified running at an apparent molecular weight of about 15 kDa (data not shown).

The strain containing the wild-type *napEDABC* cluster exhibited specific nitrate reductase activities between 0.522 and 0.987 U/mg at pH 6.5 with an average of 0.73 U/mg (four independent experiments, see Table 2). One activity unit U is defined as 1 μ mol nitrite formed per minute at 37 °C and at pH 6.5.

Table 2
Specific nitrate reductase activity of wild-type, *nap*-deficient, and mutant strains

| Strain | Specific nitrate reductase activity in different independent experiments (U/mg) | | | | Average activity (U/mg) | Percentile activity (%) | Specific FDH activity (U/mg) |
|--------------------------------------|---|-------|-------|-------|-------------------------|-------------------------|------------------------------|
| | 1 | 2 | 3 | 4 | | | |
| Wild-type Nap | 0.522 | 0.859 | 0.987 | 0.563 | 0.73 | \equiv 100 | 0 |
| Mutant C181S | 0 | 0 | 0 | — | 0 | 0 | n.d. |
| Mutant M182H | 0 | 0 | 0 | — | 0 | 0 | 0 |
| Mutant D196G | 0 | 0 | 0 | — | 0 | 0 | 0 |
| Mutant E197A | 0.597 | 0.517 | 0.410 | — | 0.51 | 70 | 0 |
| Mutant D196G,E197A | 0 | 0 | 0 | — | 0 | 0 | 0 |
| Mutant R421E | 0 | 0 | 0 | — | 0 | 0 | n.d. |
| Mutant R421K | 0.278 | 0.079 | — | — | 0.18 | 25 | n.d. |
| <i>nap</i> -Deficient strain (HF210) | 0 | 0 | 0 | — | 0 | 0 | 0 |

The different strains were grown in two to four independent experiments, periplasm was prepared, and the specific nitrate reductase activity in the periplasm was determined. The data for the wild-type NAP and the *nap*-deficient strain HF210 have been published before [16]. The formate dehydrogenase activity was analysed in only one periplasmic sample per mutant strain or in two independently grown samples for the strain harboring the wild-type *nap* cluster. n.d., not determined. Three of the strains had not been tested for FDH activity because the amino acid exchanges decrease and not increase the similarity to FDH.

| | | | |
|-----|--|-----|---------------------------|
| 166 | KAGFRSNNIDPNARHCMASAAAGFMRTFGMDEPMGCYDDFEAADA | 212 | <i>R.eutropha</i> NAP |
| 166 | RAGFRSNNLDPNARHCMASAAATAFMRTFGMDEPMGCYDDFEAADA | 212 | <i>Rh.sphaeroides</i> NAP |
| 164 | KAGFRSNNIDPNARHCMASAVVGFMRTEGMDEPMGCYDDIEQADA | 210 | <i>E. coli</i> NAP |
| 125 | KGFGTNNVGNPRLCMASAVGGYVTSFGKDEPMGTADIDQATCF | 171 | <i>D.desulf.</i> NAP |
| 182 | RS-LGMLAVDNQARVXHGPTVASLAPTFGRGAMTNHWVDIKNANVVM | 227 | <i>E.coli</i> FDH-N |
| 179 | RS-LGLFYIEHQARIKXSATVAALAESYGRGAMTNHWIDLKNSDVIL | 224 | <i>D.gigas</i> FDH |
| 125 | RAVIGTNNVDCCARVXHGPSVAGLHQSVGNGAMSNAINEIDNTDLVF | 171 | <i>E.coli</i> FDH-H |
| •• | | | |
| 390 | VYNLHLLTGKLTATPGNSPFSLTGQPSACGTAREVGTFSHRLPADMVVTN | 438 | <i>R.eutropha</i> NAP |
| 390 | VYNLHLLTGKLTSEPGNSPFSLTGQPFACGTAREVGTFAHRLPADMVVTN | 438 | <i>Rh.sphaeroides</i> NAP |
| 387 | VYNLHLLTGKLTSPGCGPFSLTGQPSACGTAREVGTFAHRLPADMVVTN | 435 | <i>E. coli</i> NAP |
| 323 | IHNLHLLTGKLTCPGATSFSLTGQENACGGVDDGGALSLLPAGRAIPN | 371 | <i>D.desulf.</i> NAP |
| 425 | MAMIQLLLGNMGMAGGGVNALRGHSNIQGLT-DLGLLSTSLFEGYLTLP | 472 | <i>E.coli</i> FDH-N |
| 421 | MSINQLLLGNIGVAGGGVNALRGEANVQGST-DHGLLMHIYEGYLTAR | 468 | <i>D.gigas</i> FDH |
| 312 | LTSLAMLTGKLPKPHAGVNPVRGQNNVQCAC-DMGALPDTYEGYQYVKD | 359 | <i>E.coli</i> FDH-H |
| • | | | |

Fig. 2. Partial homology comparison of the amino acid sequences of the catalytic α -subunits from four periplasmic nitrate reductases and from three formate dehydrogenases. Amino acids conserved in the periplasmic nitrate reductases are highlighted by black font on dark grey background, amino acids conserved in formate dehydrogenases only are highlighted by black font on light grey background. The residues conserved in both FDHs and NAPs are highlighted by white font on black background. Amino acids that were exchanged in this study are marked by dots (•). The numbers to the left and right of each sequence denote the number of the first and the last amino acids in the shown sequence. The seleno-cysteine found in the FDHs is abbreviated by an X.

From the mutants referring to amino acids in the direct vicinity of the active site, the strain with the amino acid exchange R421K showed activity values between 0.079 and 0.278 U/mg with an average of 0.179 U/mg (two independent experiments). This corresponds to an activity of the R421K mutant relative to the wild-type of $(25 \pm 14)\%$ (comparison of the mean values). The strain carrying the *nap* cluster with the mutation R421E as well as the exchange C181S showed no nitrate reductase activity (three independent experiments), nor did the *nap*-negative strain HF210 which served as a negative control (three independent experiments). R421 is believed to bind the nitrate molecule in the active site and electrostatic effects must have an important role. In fact, replacement of Arg by another positively charged amino acid (Lys) results in a significantly reduced, but measurable, nitrate reductase activity. However, replacing the positively charged Arg by a negatively charged amino acid (Glu) results in complete loss of activity as expected, although the enzyme is present in normal amounts in the periplasm as was confirmed by Western blot analysis (see Fig. 1). Replacement of Cys, which directly binds the Mo atom, by Ser at position 181 changes the coordination of Mo from sulphur to oxygen. Obviously, this is not tolerated and results in complete loss of activity.

Amino acids in the funnel leading to the active centre were exchanged at three positions. Only the strain carrying the exchange E197A showed activity values between 0.410 and 0.597 U/mg with an average of 0.508 U/mg (three independent experiments). This corresponds to an activity of the E197A mutant relative to the wild-type of $(70 \pm 14)\%$ (comparison of the mean values). The strains with the exchanges D196G, M182H and the

double mutant “DEGA” (D196G-E197A) showed no nitrate reductase activity.

Discussion

The purified periplasmic nitrate reductase from *D. desulfuricans* exhibits a small cross activity as formate dehydrogenase [27]. The activity amounts to only 1 mU/mg and therefore differs by four orders of magnitude from the specific nitrate reductase activity [5]. In an analogous manner the formate dehydrogenase from *D. desulfuricans* showed a slight nitrate reductase activity [5]. This cross activity is not surprising, since periplasmic nitrate reductases and formate dehydrogenases exhibit a great structural similarity, the major differences occurring at the active site and in the funnel through which the substrate accesses the active site (see Fig. 3).

We thus speculated that amino acid exchanges replacing amino acids conserved in NAPs by amino acids conserved in FDHs will enhance this cross activity. In a first step we mutated amino acids at the active site in the direct vicinity of the molybdenum and studied their influence on the nitrate reductase activity. In a second step we exchanged highly conserved amino acids in the substrate funnel by the corresponding conserved amino acids from FDHs.

Recently, we constructed a three-dimensional model of the catalytic subunit NAP-A from *R. eutropha* (*R.eu.NAP-A*) based on the *D. desulfuricans* structure (*D.d.NAP*) [5,16]. The major sequence differences between the two structures, the two loops in the *Ralstonia* enzyme, are located at the protein surface. The func-

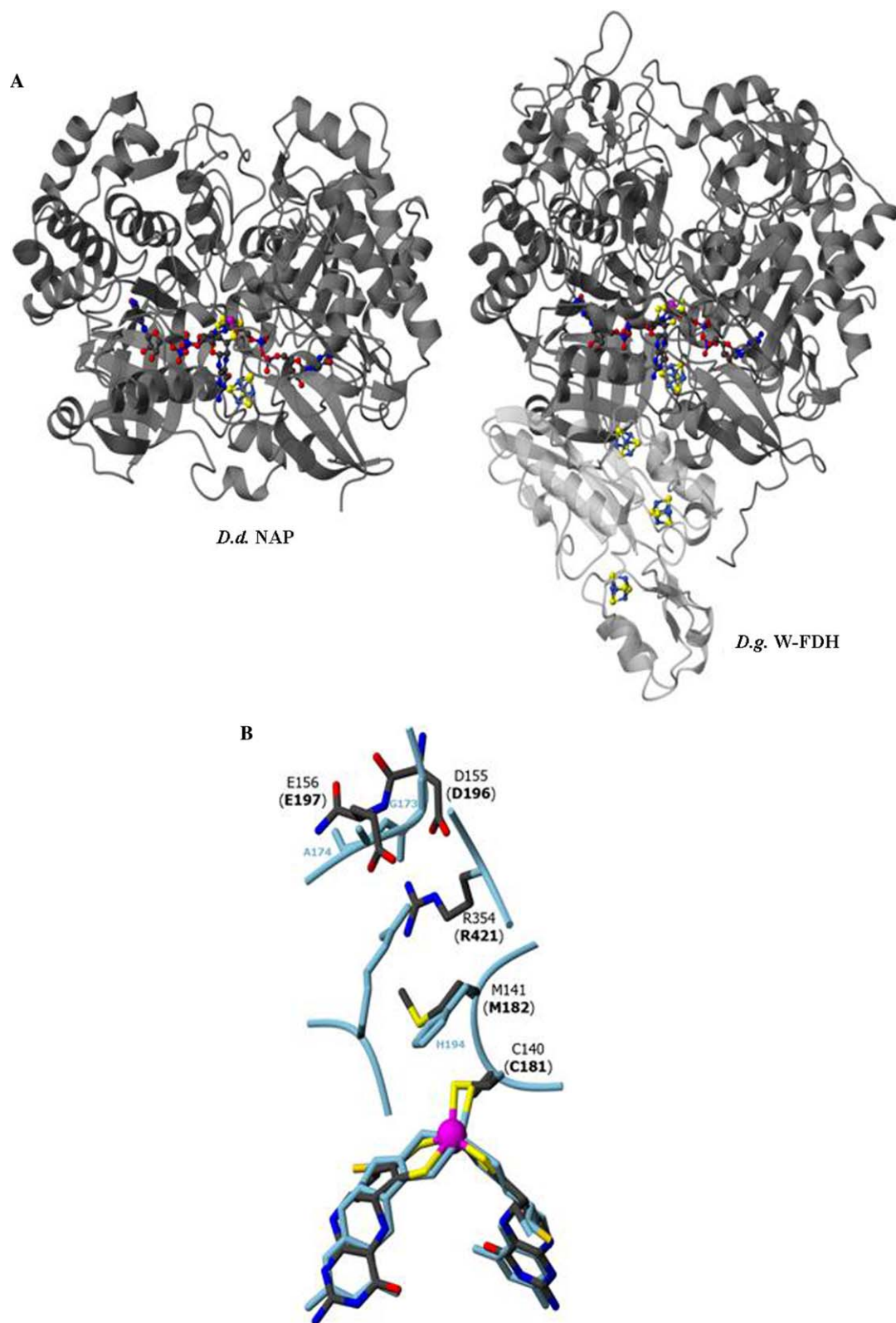


Fig. 3. (A) Overall structures of *D. desulfuricans* NAP and *D. gigas* W-FDH. W-FDH α are shown in dark grey, W-FDH β in light grey. The Mo-bisMGD and FeS cluster are represented as colour coded ball-and-sticks and Mo/W in purple. (B) Superpositioning of the molybdenum catalytic site and surrounding residues of *D.d.*NAP (in colour code) and of *D.g.*W-FDH (in blue) and amino acid residues replaced in the course of this mutational study. Residues numbering correspond to *D.d.*NAP and those in parentheses to the corresponding amino acids in *R.e.*NAPA. (For interpretation of the references to color in this figure legend, the reader is referred to the web version of this paper.)

tionally relevant protein parts required for catalytic nitrate reduction as compared to the *D.d.*NAP remain nearly unmodified (see Fig. 1B in [16]). Thus, the molybdenum active site is accessible from the surface through the funnel-like cavity, a structural feature also common to the other molybdopterin-containing enzymes. In *R.eu.*NAP-A, as in *D.d.*NAP, a cysteine residue binds to the Mo atom, and the nitrate molecule is presumably positioned by Arg421 (Arg354 in *D.d.*) for catalysis to take place. The entrance from the wider part of the tunnel leading to the molybdenum is coated with polar residues: Arg421 and Asp196 point downwards and form a salt bridge, Glu197 and Glu422 are at mid-height. Towards the surface there is a patch of hydrophobic residues. Several ordered water molecules in the wide-open part of the cavity contact the bulk solvent. We used this structural model as the basis for our mutagenesis studies.

Exchange of the molybdenum coordinating amino acid

The exchange of the amino acid residue ligating the Mo atom from a cysteine (C181) to a serine resulted in a complete loss of nitrate reductase activity, underlining the importance of Mo complexation by sulphur. In formate dehydrogenase, the role of C181 is taken over by a seleno-cysteine. The exchange of C181 to seleno-cysteine (a consequent next step in our mutagenesis studies) requires, however, a complex incorporation mechanism and is thus not included in this study.

Amino acid exchanges in the funnel leading to the active site

We then studied amino acid residues conserved within the periplasmic nitrate reductase family and located in the funnel which leads to the active site. The positively charged arginine R421 is thought to correctly position the negatively charged nitrate during the reaction cycle. The results of the exchanges of the residue R421 to lysine and to glutamate can be explained on an electrostatic basis: lysine, another positively charged amino acid, can—to some extent—take over the role of arginine. The exchange R421K showed an average activity of 25% compared to the wild-type NAP. An exchange to the negatively charged amino acid glutamate, however, leads to a complete loss of nitrate reductase activity, thus hinting at the significant role of a positive charge to hold the substrate molecule nitrate in the correct position. In FDH, R421 has no corresponding amino acid (see alignment in Fig. 2).

The three mutated residues D196, E197, and M182 in the substrate funnel are highly conserved in periplasmic nitrate reductases (Fig. 2).

Obviously, they are not equally important for nitrate reductase activity. The exchanges M182H, D196G and

the double exchange D196G-E197A resulted in a complete loss of nitrate reductase activity. The carboxylate of residue D196 forms a salt bridge with residue R421 [5,6] (Fig. 3). The exchange of D196 to the small uncharged glycine residue putatively destroys this salt bridge and disrupts the structure of the entrance to the funnel.

Residue E197, however, is not as important as the other residues examined. The exchange to the uncharged alanine residue resulted in a mediocre decrease of nitrate reductase activity exhibiting 70% of wild-type activity.

In contrast to D196, the residue E197 does not form a salt bridge with another amino acid. The different behaviours of these two amino acids in the mutagenesis experiments hint at the importance of intramolecular salt bridges for building the active enzyme structure.

Neither of these mutant strains exhibited an FDH activity detectable with our assay. It could well be that the amino acid essential for FDH specific activity has not been identified and analysed yet. Probably, the mutational exchange pattern has to be more complex than the design of our initial experiments presented here, including both, the funnel and the active site.

From an evolutionary point of view it could be speculated that the oxidoreductase enzyme family is constructed from three elements: (i) the electron transport to the active site, (ii) the active site carrying out the chemical reaction, and (iii) the substrate funnel regulating the substrate specificity, all three of which may be viewed rather independently. The cross activity of the nitrate and formate dehydrogenase activity—although being small—supports the thesis that not the active site—but may be the funnel—determines substrate specificity. Recently we analysed the function of the conserved Lys positioned between the Fe-S-centre and the pterin [16]. We found that this Lys can be replaced by another positively charged amino acid (Arg) resulting in a reduced nitrate reductase activity (23% relative to wild-type), however, not by a polar uncharged residue (Met [16]). In line with this hypothesis, we would speculate that this part of the enzyme is involved neither in the chemical reaction nor in substrate specificity. In the results presented here, we observe that the active site is rather intolerant to the mutation of the amino acid coordinating the Mo. The correct complexation of the Mo is thus essential. Furthermore, we find that the mutations of conserved amino acids in the funnel do not, at least not measurably by our assay, increase the FDH activity of the mutated nitrate reductase. Thus, viewing the enzyme as a unit constructed from three rather independent blocks with separate functions is certainly over-simplified and the transfer of the nitrate to a formate dehydrogenase activity is more complex than the above-mentioned hypothesis would predict.

These first experiments will, however, build the basis for further amino acid exchanges which are currently

under way and will hopefully elucidate the factors determining the substrate specificity of NAP and FDH.

Acknowledgments

We thank the DFG for funding our work (SFB 436, Project B7). M.J.R. thanks the Alexander von Humboldt Foundation for a follow-up fellowship. We thank José Trincão for helping with the figures.

Note added in proof. The strain *Ralstonia eutropha* has recently been reclassified as *Wautersia eutropha* [30].

References

- [1] M. Bertero, R. Rothery, M. Palak, C. Hou, D. Lim, F. Blasco, J. Weiner, N. Strynadka, Insights into the respiratory electron transfer pathway from the structure of nitrate reductase A, *Nat. Struct. Biol.* 10 (9) (2003) 681–687.
- [2] M. Jormakka, D. Richardson, B. Byrne, S. Iwata, Architecture of NarGH reveals a structural classification of Mo-bisMGD enzymes, *Structure (Camb.)* 12 (1) (2004) 95–104.
- [3] D.J. Richardson, B.C. Berks, D.A. Russell, S. Spiro, C.J. Taylor, Functional, biochemical and genetic diversity of prokaryotic nitrate reductases, *Cell. Mol. Life Sci.* 58 (2) (2001) 165–178.
- [4] R. Hille, The mononuclear molybdenum enzymes, *Chem. Rev.* 96 (7) (1996) 2757–2816.
- [5] J.M. Dias, M.E. Than, A. Humm, R. Huber, G.P. Bourenkov, H.D. Bartunik, S. Bursakov, J. Calvete, J. Caldeira, C. Carneiro, J.J. Moura, I. Moura, M.J. Romão, Crystal structure of the first dissimilatory nitrate reductase at 1.9 Å solved by MAD methods, *Structure Fold. Des.* 7 (1) (1999) 65–79.
- [6] M.J. Romão, J.M. Dias, I. Moura, Dissimilatory nitrate reductase (NAP), in: K. Wieghardt, R. Huber, T.L. Poulos, A. Messerschmidt (Eds.), *Handbook of Metalloproteins*, Wiley-VCH, New York, 2001, pp. 1075–1085.
- [7] A. Brigé, D. Leys, T.E. Meyer, M.A. Cusanovich, J.J. Van Beeumen, The 1.25 Å resolution structure of the diheme NapB subunit of soluble nitrate reductase reveals a novel cytochrome *c* fold with a stacked heme arrangement, *Biochemistry* 41 (15) (2002) 4827–4836.
- [8] P. Arnoux, M. Sabaty, J. Alric, B. Frangioni, B. Guigliarelli, J. Adriano, D. Pignol, Structural and redox plasticity in the heterodimeric periplasmic nitrate reductase, *Nat. Struct. Biol.* 10 (11) (2003) 928–934.
- [9] J.C. Boyington, V.N. Gladyshev, S.V. Khangulov, T.C. Stadtman, P.D. Sun, Crystal structure of formate dehydrogenase H: catalysis involving Mo, molybdopterin, selenocysteine, and an Fe₄S₄ cluster, *Science* 275 (5304) (1997) 1305–1308.
- [10] M. Jormakka, S. Tornroth, B. Byrne, S. Iwata, Molecular basis of proton motive force generation: structure of formate dehydrogenase-N, *Science* 295 (5561) (2002) 1863–1868.
- [11] H. Raaijmakers, S. Teixeira, J.M. Dias, M.J. Almendra, C.D. Brondino, I. Moura, J.J. Moura, M.J. Romão, Tungsten-containing formate dehydrogenase from *Desulfovibrio gigas*: metal identification and preliminary structural data by multi-wavelength crystallography, *J. Biol. Inorg. Chem.* 6 (4) (2001) 398–404.
- [12] H. Raaijmakers, S. Macieira, J. Dias, S. Teixeira, S. Bursakov, R. Huber, J. Moura, I. Moura, M. Romão, Gene sequence and the 1.8 Å crystal structure of the tungsten-containing formate dehydrogenase from *Desulfovibrio gigas*, *Structure (Camb.)* 10 (9) (2002) 1261–1272.
- [13] U. Warnecke-Eberz, B. Friedrich, Three nitrate reductase activities in *Alcaligenes eutrophus*, *Arch. Microbiol.* 159 (1993) 405–409.
- [14] C. Kortlüke, K. Horstmann, E. Schwartz, M. Rohde, R. Binsack, B. Friedrich, A gene complex coding for the membrane-bound hydrogenase of *Alcaligenes eutrophus* H16, *J. Bacteriol.* 174 (19) (1992) 6277–6289.
- [15] R.A. Siddiqui, U. Warnecke-Eberz, A. Hengsberger, B. Schneider, S. Kostka, B. Friedrich, Structure and function of a periplasmic nitrate reductase in *Alcaligenes eutrophus* H16, *J. Bacteriol.* 175 (18) (1993) 5867–5876.
- [16] T. Hettmann, R.A. Siddiqui, J. von Langen, C. Frey, M.J. Romão, S. Diekmann, Mutagenesis study on the role of a lysine residue highly conserved in formate dehydrogenases and periplasmic nitrate reductases, *Biochem. Biophys. Res. Commun.* 309 (2003) 40–47.
- [17] H.G. Schlegel, H. Kaltwasser, G. Gottschalk, Ein Submersverfahren zur Kultur wasserstoffoxidierender Bakterien: wachstumsphysiologische Untersuchungen, *Arch. Mikrobiol.* 38 (1961) 209–222.
- [18] S. Sambrook, E.F. Fritsch, T. Maniatis, *Molecular Cloning: A Laboratory Manual*, second ed., Cold Spring Harbor Laboratory, Cold Spring Harbor, NY, 1989.
- [19] C.J. Marx, M.E. Lidstrom, Development of improved versatile broad-host-range vectors for use in methylotrophs and other Gram-negative bacteria, *Microbiology* 147 (2001) 2065–2075.
- [20] M. Bernhard, B. Friedrich, R.A. Siddiqui, *Ralstonia eutropha* TF93 is blocked in tat-mediated protein export, *J. Bacteriol.* 182 (3) (2000) 581–588.
- [21] H. Borchering, S. Leikefeld, C. Frey, S. Diekmann, P. Steinrück, Enzymatic microtiter plate-based nitrate detection in environmental and medical analysis, *Anal. Biochem.* 282 (1) (2000) 1–9.
- [22] O.H. Lowry, N.J. Rosebrough, A.L. Farr, R.J. Randall, Protein measurement with the folin phenol reagent, *J. Biol. Chem.* 193 (1951) 265–275.
- [23] U.K. Laemmli, Cleavage of structural proteins during the assembly of the head of bacteriophage T4, *Nature* 227 (1970) 680–685.
- [24] J.D. Thompson, D.G. Higgins, T.J. Gibson, CLUSTAL W: improving the sensitivity of progressive multiple sequence alignment through sequence weighting, position-specific gap penalties and weight matrix choice, *Nucleic Acids Res.* 22 (22) (1994) 4673–4680.
- [25] C. Combet, C. Blanchet, C. Geourjon, G. Deleage, NPS@: network protein sequence analysis, *Trends. Biochem. Sci.* 25 (3) (2000) 147–150.
- [26] E. Schwartz, A. Henne, R. Cramm, T. Eitinger, B. Friedrich, G. Gottschalk, Complete nucleotide sequence of pHG1: a *Ralstonia eutropha* H16 megaplasmid encoding key enzymes of H(2)-based lithoautotrophy and anaerobiosis, *J. Mol. Biol.* 332 (2) (2003) 369–383.
- [27] S.A. Bursakov, C. Carneiro, M.J. Almendra, R.O. Duarte, J. Caldeira, I. Moura, J.J. Moura, Enzymatic properties and effect of ionic strength on periplasmic nitrate reductase (NAP) from *Desulfovibrio desulfuricans* ATCC 27774, *Biochem. Biophys. Res. Commun.* 239 (3) (1997) 816–822.
- [28] R. Simon, U. Priefer, A. Pühler, A broad host range mobilization system for in vivo genetic engineering: transposon mutagenesis in Gram-negative bacteria, *Biotechnology* 1 (1983) 784–791.
- [29] V.C. Knauf, E.W. Nester, Wide host range cloning vectors: a cosmid clone bank of an *Agrobacterium* Ti plasmid, *Plasmid* 8 (1) (1982) 45–54.
- [30] M. Vaneechoutte, P. Kampfer, T. De Baere, E. Falsen, G. Verschraegen, *Wautersia gen. nov.*, a novel genus accommodating the phylogenetic lineage including *Ralstonia eutropha* and related species, and proposal of *Ralstonia [Pseudomonas] syzygii comb. nov.*, *Int. J. Syst. Evol. Microbiol.* 54 (2004) 317–327.